Journal of Biomechanics 49 (2016) 4119–4123

Contents lists available at ScienceDirect

Journal of Biomechanics

journal homepage: www.elsevier.com/locate/jbiomech
www.JBiomech.com

Short communication

A new validation technique for estimations of body segment inertia tensors: Principal axes of inertia do matter

Marcel M. Rossi [a], Jacqueline Alderson [a], Amar El-Sallam [a], James Dowling [b], Jeffrey Reinbolt [c], Cyril J. Donnelly [a,*]

[a] School of Sport Science, Exercise and Health, The University of Western Australia, Perth, Australia
[b] Department of Kinesiology, McMaster University, Hamilton, Canada
[c] Mechanical, Aerospace, and Biomedical Engineering Department, University of Tennessee, Knoxville, USA

ARTICLE INFO

Article history:
Accepted 9 October 2016

Keywords:
Validation
Simulation
Compound pendulum
Criterion method
Anthropometry
Airborne motion

ABSTRACT

The aims of this study were to: (i) establish a new criterion method to validate inertia tensor estimates by setting the experimental angular velocity data of an airborne objects as ground truth against simulations run with the estimated tensors, and (ii) test the sensitivity of the simulations to changes in the inertia tensor components. A rigid steel cylinder was covered with reflective kinematic markers and projected through a calibrated motion capture volume. Simulations of the airborne motion were run with two models, using inertia tensor estimated with geometric formula or the compound pendulum technique. The deviation angles between experimental (ground truth) and simulated angular velocity vectors and the root mean squared deviation angle were computed for every simulation. Monte Carlo analyses were performed to assess the sensitivity of simulations to changes in magnitude of principal moments of inertia within $\pm 10\%$ and to changes in orientation of principal axes of inertia within $\pm 10°$ (of the geometric-based inertia tensor). Root mean squared deviation angles ranged between 2.9° and 4.3° for the inertia tensor estimated geometrically, and between 11.7° and 15.2° for the compound pendulum values. Errors up to 10% in magnitude of principal moments of inertia yielded root mean squared deviation angles ranging between 3.2° and 6.6°, and between 5.5° and 7.9° when lumped with errors of 10° in principal axes of inertia orientation. The proposed technique can effectively validate inertia tensors from novel estimation methods of body segment inertial parameter. Principal axes of inertia orientation should not be neglected when modelling human/animal mechanics.

1. Introduction

The inertia tensor is an inertial property of body segments that expresses mathematically how mass is distributed about the segment's reference frame. This 3×3 matrix represents the link in the cause-effect relationship between torque applied to the segment and its rotational kinematics. Any inertia tensor has 3 eigenvectors with specific properties: they are orthogonal and define the only axes about which the torque applied would yield rotation about the axis alone. These axes are the principal axes of inertia, and their respective moments of inertia are the principal moments of inertia. Thus, assessment of inertia tensors accuracy is given by measuring discrepancies in orientation of principal axes of inertia and magnitude of principal moments of inertia against some ground truth value.

The compound pendulum (CP) is currently the gold standard method for validating moments of inertia and inertia tensor estimates of biological specimens from medical imaging technologies (Huang and Suarez, 1983; Ackland et al., 1988; Martin et al., 1989; Durkin et al., 2002). Yet, the CP method relies in the accuracy of several independent variables measured experimentally (Dowling et al., 2006). With errors of up to 15% reported for moments of inertia estimations, the application of CP for validation purposes can be questioned (Durkin et al.; 2002, Dowling et al., 2006).

In the field of Biomechanics, it is conventional to estimate the moments of inertia about the anatomical coordinate system axes

Abbreviations: CP, Compound Pendulum: method to estimate experimentally the moments of inertia and the inertia tensor of an object under suspended oscillation; DA, Deviation Angle: angle measured between two sampled angular velocity vectors, one from experimental and other from simulated data; GF, Geometric Formulae: Formulae using dimensions of homogeneous objects with perfect geometry to compute the moments of inertia and the inertia tensor of the object; CCS, Cylinder Coordinate System: reference frame with respect to which the inertia tensor of the cylinder was estimated.

* Correspondence to: School of Sport Science, Exercise and Health – The University of Western Australia (M408) 35 Stirling Highway, Crawley Perth, Western Australia 6009 – Australia. Fax: +61 8 6488 1039.
E-mail address: cyril.donnelly@uwa.edu.au (C.J. Donnelly).

http://dx.doi.org/10.1016/j.jbiomech.2016.10.006
0021-9290/

instead of the inertia tensor. This is under the assumption anatomical axes are aligned with the principal axes of inertia of segment, so more simplified biomechanical models and equations of motion can be employed (Andrews, 1995; Zatsiorsky, 2002). Few studies reported deviation of the principal axes of inertia from the anatomical axes, which can be as large as 10° for the longitudinal axis (Chandler et al., 1975; McConville et al., 1980). It remains unclear, however, how these deviations may affect human dynamics investigations (Zatsiorsky, 2002).

As solution to the abovementioned problems, consider a rigid body with estimated inertia tensor rotating airborne. Simulations of this motion would only match the experimental kinematics (ground truth) if the inertia tensor used with the simulation model is accurate. Airborne rotations are torque-free, with orientation of the angular velocity vector changing in time. Differences in orientation between a sampled experimental angular velocity vector and the corresponding simulated can be measured as deviation angle (DA) between the vectors. Hence, the smaller the observed DA data, the smaller the errors in magnitude of principal moments of inertia, orientation of the principal axes of inertia, or a combination of both.

We then set two hypothesis. Firstly, simulations of flying objects with known geometry would yield significantly larger DA data if run with the inertia tensor estimated with CP instead of geometric formulae. Secondly, DA data would be sensitive to changes in the inertia tensor components. Acceptance of the first hypothesis will lead into establishing a new criterion method to validate inertia tensor by setting the experimental angular velocity data as ground truth against simulations run with the estimated tensor, whereas acceptance of the second hypothesis will reveal the relevance of the orientation of the principal axes of inertia to the accuracy of inertia tensor estimation.

2. Methods

A homogeneous steel cylinder (mass = 10.010 ± 0.001 kg) was measured with a high precision calliper (height = 97.0 ± 0.2 mm, diameter = 129.8 ± 0.3 mm). A local coordinate system (CCS) was created, with origin at the centre of the cylinder's volume and defining three planes of symmetry (one parallel to the cylinder's base).

The inertia tensor of the cylinder relative to CCS was calculated with the compound pendulum (CP) technique and also with geometric formulae (GF) using the cylinder's dimensions and mass as predictors (Dowling et al., 2006). Both techniques adopted the CCS axes as the cylinder's principal axes of inertia, then only the principal moments of inertia about the sagittal (**X**), transverse (**Y**) and longitudinal (**Z**) axes were estimated. The required experimental trials for the CP method (Appendix A) were recorded with the 12-camera Vicon MX system (Oxford Metrics, Oxford, UK) at 250 Hz.

Four retro-reflective kinematic markers (12 mm diameter) were adhered to the cylinder's surface. The cylinder was manually projected in the air to allow for its rotation about an axis non-parallel to the CCS axes. All marker positions were recorded throughout the airborne motion (from first frame after release till last frame before hitting the ground) with the 12-camera Vicon MX system (250 Hz).

The marker trajectories were imported into OpenSim (v. 3.3, simt-k.org, Stanford, CA). The experimental kinematics time history of the motion (i.e., Cartesian position of the model origin, the Cardan angles of the model coordinate system and their respective derivatives), was output by the inverse kinematics tool, with enhanced sampling rate of 1,000 Hz.

The OpenSim Application Programming Interface (API) was run in Matlab (v. 7.8.0, The Math Works, Natick, Massachusetts) to simulate the cylinder airborne motion (solution through integration of the Newton-Euler differential equations that define the dynamics of the model), using one model with CP-based inertia tensor and another model with GF data (Fig. 1). Every sampled data from the experimental kinematics was used as initial states to run the simulations. To account for the whole flight time, simulations were also run backwards in time, later inverted and bound to the correspondent simulation forward in time. A total of 873, full-flight simulations were run for each model (total flight time = 0.872 s).

The time histories of the angular velocity vectors of the experimental kinematics and all simulations were calculated with a custom Matlab function. The function used the time histories of the Cardan angles output by the inverse kinematics (experimental) and the forward dynamics (simulations) tools to recover the time history of the model's rotation matrix. Then, each pair of consecutive rotation matrices defined an instantaneous axis of rotation, which expressed the orientation of a sampled angular velocity vector according to the Euler's rotation theorem.

The angular velocity data from the experimental kinematics (ground truth) and from a given simulation were compared by calculating the deviation angle (DA) time history (degrees) and the Root Mean Squared DA, with custom Matlab functions. Boxplot figures (10th–90th percentile) summarised the Root Mean Squared DA of all simulations run with each model.

The sensitivity of DA data to changes in magnitude and orientation of principal moments and axes of inertia, respectively, were investigated with Monte Carlo probabilistic analyses. For each analysis, the OpenSim API run in Matlab was used to create a domain of 5,000 inertia tensors within a range of allowable bounds (from a uniform distribution of pseudorandom numbers). Twelve ranges of allowable bounds were chosen, yielding twelve analyses: ± 2.5%, ± 5%, ± 7.5% and ± 10% of the values computed with GF for variations in principal moments of inertia; ± 2.5°, ± 5°, ± 7.5° and ± 10° from the respective CCS axes for variations in orientation of principal axes of inertia; and the combination of the corresponding ranges for variations in principal moments and axes of inertia simultaneously. Thus, 5,000 simulations were run for each analysis from randomly sampled initial state, with boxplot figures (10th–90th percentile) summarising all computed Root Mean Squared DA (Fig. 2).

3. Results

Table 1 numerically compares the principal moments of inertia estimated with GF and CP. The Root Mean Squared DA for

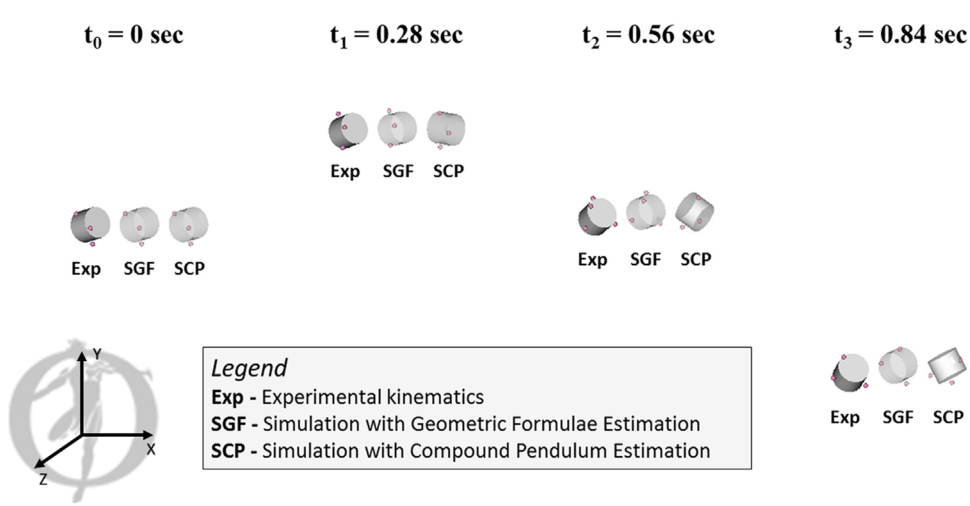

Fig. 1. Orientation of three cylinder models at four different sampled instants during the airborne motion (t_0, t_1, t_2 and t_3). The first model was animated with the experimental kinematics (Exp) run with the Inverse Kinematics tool in OpenSim. With each of the other two models featuring inertia tensor estimated with Geometric Formulae or the Compound Pendulum methods, simulations were run to animate the models (SGF and SCP, respectively) in OpenSim Application Program Interface (API) run in Matlab. The exemplified simulation was run using the data sampled at instant t_1 from the experimental kinematics as initial state.

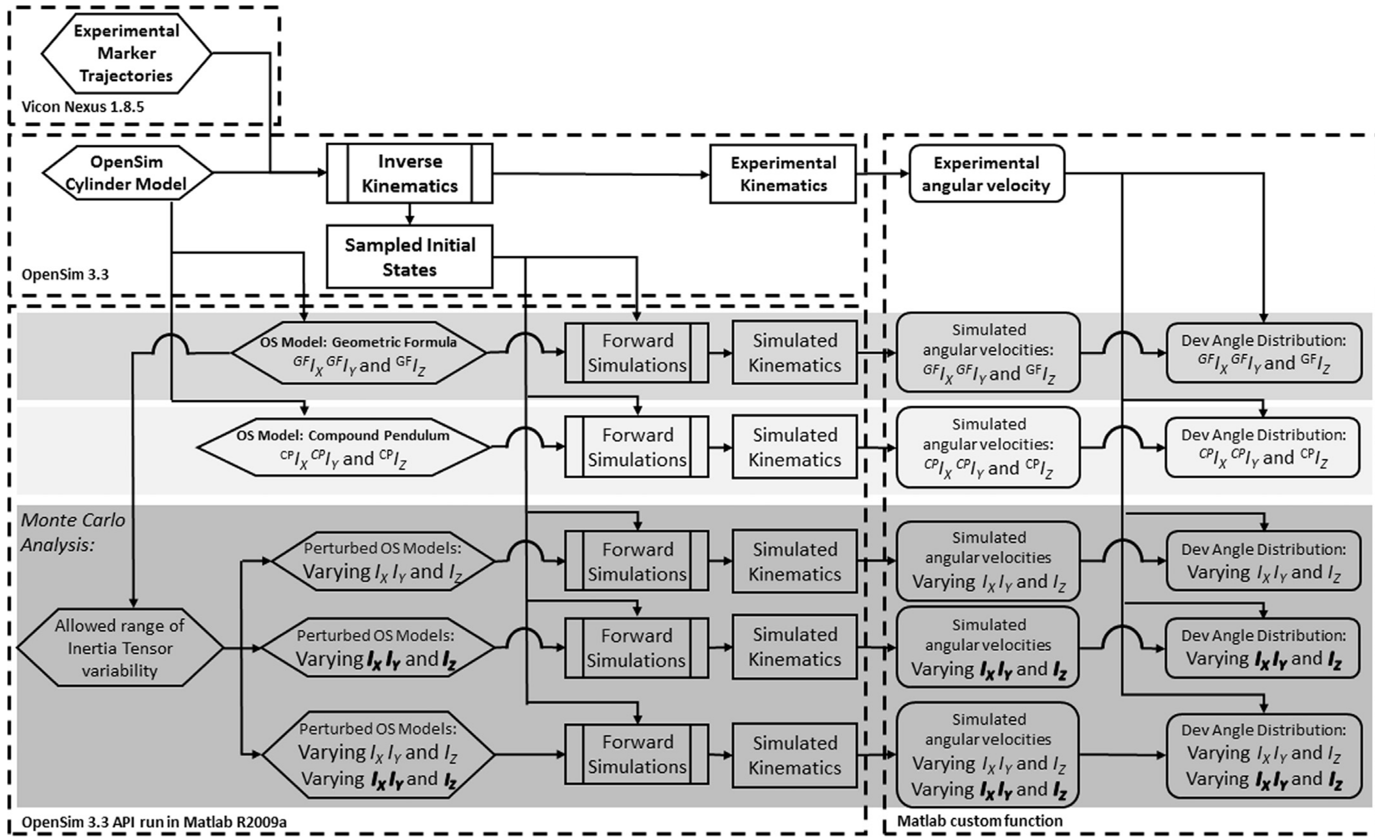

Fig. 2. Flow chart describing all analyses carried out in the present study. The Inverse Kinematics tool in OpenSim (OS) used the experimental marker trajectories of the cylinder recorded with Vicon Nexus to output the ground-truth experimental kinematics. The sampled experimental kinematics were also used as initial states to simulate the cylinder flight in OpenSim API run in Matlab. To test the first hypothesis, simulations were run using models featuring principal moments of inertia computed with geometric formulae (${}^{GF}I_X$, ${}^{GF}I_Y$ and ${}^{GF}I_Z$) and estimated with the compound pendulum method (${}^{CP}I_X$, ${}^{CP}I_Y$ and ${}^{CP}I_Z$). To test the second hypothesis, perturbed models with varying magnitudes in principal moments of inertia (I_X, I_Y and I_Z) and orientation of principal axes of inertia (I_X, I_Y and I_Z) were created through Monte Carlo Analysis in OpenSim Application Program Interface (API), within ranges of allowable bounds. Matlab custom functions were used to (i) calculate the time history of angular velocity vectors from the ground-truth experimental kinematics and every simulation and (ii) compare the orientations of the experimental and the simulated angular velocity vectors by measuring the deviation angles and the root mean squared deviation angle for each simulation.

simulations run with the GF values ranged between 2.9° and 4.3° (10th–90th percentile), with median of 3.1°, whereas for CP values the observed range was between 11.7° and 15.2°, with median of 13.5°.

Root Mean Squared DA distribution gradually increased across percentage of allowable bounds of principal moments of inertia, reaching between 3.2° and 6.6° (median = 4.4°) at 100% of allowable bound. This increase was more pronounced when combined with variations in orientation of principal moments and axes of inertia, reaching between 5.5° and 7.9° (median = 6.4°) at 100% of allowable bound. Variation in just principal axes of inertia orientation at 100% of allowable bound reached between 3.0° and 4.4° (median = 3.3°).

4. Discussion

Our first hypothesis was confirmed, with results showing simulations run with CP-based inertia tensor estimates produce significantly larger DA data than the simulations with inertia tensor estimates derived mathematically from a geometric formula. As the geometric estimates were computed from a perfectly homogeneous rigid cylinder, the observed DA were likely due to systematic errors during 3D stereoscopic reconstruction and the inverse kinematic modelling process. The large DA between GF and CP simulations (Fig. 3, A) were likely due to systematic errors in magnitude of the principal moments of inertia, yet these

Table 1
Cylinder principal moments of inertia (I_X, I_Y and I_Z) computed from the geometric formulae (GF) and using the compound pendulum technique (CP), with their respective uncertainties (μ). Errors from the CP method are expressed as percentage of the GF values.

	GF ± μ	CP ± μ	Error (% Criteria) (%)
I_X (kg cm^2)	183.8 ± 0.6	203.3 ± 12.4	10.56
I_Y (kg cm^2)	183.8 ± 0.6	155.0 ± 9.0	−15.66
I_Z (kg cm^2)	210.8 ± 0.5	192.5 ± 34.4	−8.66

systematic errors (Table 1) were in accordance with values previously reported in the literature (Durkin et al., 2002). Therefore, inertia tensor estimations can be validated by comparing simulations of an airborne rigid object against the ground-truth experimental kinematics. This method is an effective alternative to concurrent validation against CP-based estimations.

The above mentioned results do not suggest we should reject the CP technique to estimate moments of inertia and inertia tensor of solid objects, they only endorse its rejection as gold standard for validation purposes (Dowling et al., 2006). According to Dowling et al. (2006), the moment of inertia of irregularly-shaped, non-homogeneous objects can be accurately estimated with CP if the distance between the object centre of mass to the swing axis is about the same length of the object's radius of gyration. However, research dealing with merging areal density data from Dual-Energy X-Ray Absorptiometry (DXA) with different volumetric

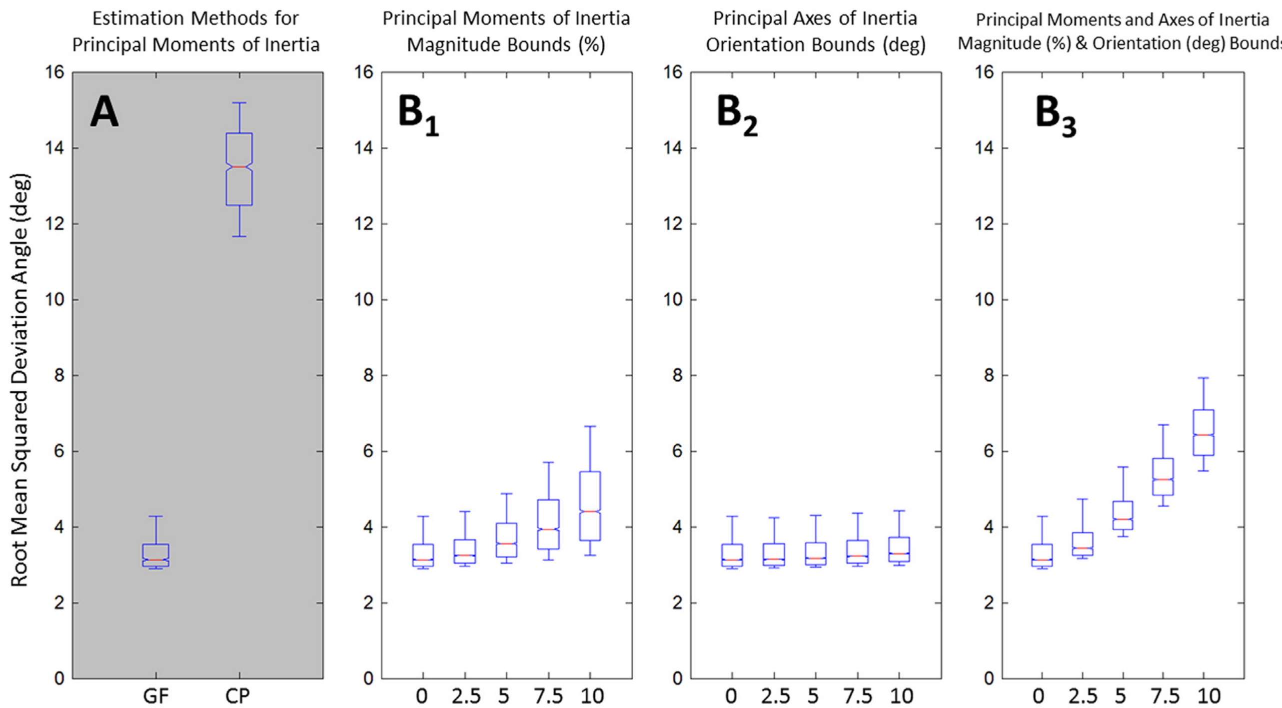

Fig. 3. Subplot A shows boxplot figures summarizing distribution of root mean squared deviation angles (deg.) of flight simulations using principal moments of inertia from the geometric formulae (GF) and the compound pendulum (CP). Boxplots summarising distribution of root mean squared deviation angles from the Monte Carlo analysis are shown in subplot B_1, B_2 and B_3. Subplot B_1 shows results for variations in magnitude of principal moments of inertia within 0%, ±2.5%, ±5%, ±7.5% and ±10% of the values found with the geometric formula; subplot B_2 shows results for variations in orientation of principal axes of inertia within 0°, ±2.5°, ±5°, ±7.5° and ±10° offset from cylinder coordinate system (CCS) axes; subplot B_3 shows results for combined variations in corresponding allowable bounds for principal moments and axes of inertia. Whiskers are set to the 10th (lowest) and 90th (highest) percentiles.

modelling techniques suggest these new approaches could estimate body segment inertia tensor more accurately than the CP method (Durkin et al., 2002; Durkin and Dowling, 2006; Lee et al., 2009; Wicke and Dumas, 2010). Our proposed technique could, for instance, determine if a new medical imaging technology better estimates the inertia tensor of a frozen cadaveric segment than the CP method.

Results from the Monte Carlo analyses demonstrate the importance of accurate orientation of the principal axes of inertia. In isolation, errors in orientation thereof did not affect the DA data (Fig. 3, B_2), because the cylinder had similar mass distribution about the principal axes. In this situation, the orientation of the principal axes becomes negligible. However, increasing errors in magnitude of principal moments of inertia yielded larger DA data (Fig. 3, B_1) and also introduced differences in mass distribution about the principal axes of inertia. These differences in mass distribution combined with errors in principal axis orientation made the DA data increase more exponentially (Fig. 3, B_3). Therefore, the greater the difference in mass distribution with respect to the principal axes of inertia, the greater the relevance of the true orientation of these axes to the accuracy of the inertia tensor. As limb segments have considerable smaller moment of inertia about the longitudinal axis, errors in orientation of their principal axis of inertia in the longitudinal direction may have a large impact in the inertia tensor accuracy, and thus should not be neglected. This may be of particular relevance when investigating upper limb, overhead throwing tasks (McConnell et al., 2011, 2012).

The meaningfulness of errors in estimated inertia tensors for human dynamic analyses, nevertheless, depends on the types of motion observed and investigation carried out (Durkin, 2008). Even when these errors are effectually irrelevant, accurate body segment inertial parameters should not be rejected if they can be easily estimated. Recent advances in medical image analysis, computer sciences and software engineering will soon allow us estimate body segment inertial properties accurately, rapidly and at minimum cost with technologies widely accessible (Durkin et al., 2002; Lee et al., 2009; Wicke and Dumas, 2010; Rossi et al., 2013). These data can then be used with more accurate computational musculoskeletal models that are currently available through open-source software platforms (Delp et al., 2007; Reinbolt et al., 2011), instead of classic, simplified biomechanical models. In this scenario, the alignment assumption between anatomical and principal axes of inertia may soon be regarded obsolete. Therefore, body segment inertia tensors must be estimated instead of anatomical moments of inertia when it is feasible to use medical imaging technologies.

Conflict of interest

There were no financial or personal relationships with other people or organizations that could have biased the presented work.

Acknowledgements

The authors would like to thank Prof. Scott Delp and the National Center for Simulation Rehabilitation Research for assisting with travel funding to work with Dr. Jeffrey Reinbolt.

Appendix A. Supplementary material

Supplementary data associated with this article can be found in the online version at http://dx.doi.org/10.1016/j.jbiomech.2016.10.006.

References

Ackland, T., Henson, P., Bailey, D., 1988. The uniform density assumption: its effect upon the estimation of body segment inertial parameters. Int. J. Sport Biomech. 4, 146–155.

Andrews, J.G., 1995. Euler's and Lagrange's equations for linked rigid-body models of three-dimensional human motion. In: Allard, P., Stokes, I.A.F., Blanchi, J.-P. (Eds.), Three-Dimensional Analysis of Human Movement. Human Kinetics, Champaign, pp. 145–175.

Chandler, R.F., Clauser, C.E., McConville, J.T., Reynolds, H.M., Young, J.W., 1975. Investigation of Inertial Properties of the Human Body, AMRL-TR-70-137. Aerospace Medical Research Laboratory, Wright-Patterson Air Force Base, Ohio.

Delp, S.L., Anderson, F.C., Arnold, A.S., Loan, P., Habib, A., John, C.T., Guendelman, E., Thelen, D.G., 2007. OpenSim: open-source software to create and analyze dynamic simulations of movement. IEEE Trans. Biomed. Eng. 54, 1940–1950.

Dowling, J.J., Durkin, J.L., Andrews, D.M., 2006. The uncertainty of the pendulum method for the determination of the moment of inertia. Med. Eng. Phys. 28, 837–841.

Durkin, J., Dowling, J., 2006. Body segment parameter estimation of the human lower leg using an elliptical model with validation from DEXA. Ann. Biomed. Eng. 34, 1483–1493.

Durkin, J.L., 2008. Measurement and estimation of human body segment parameters. In: Hong, Y., Bartlett, R. (Eds.), Routledge Handbook of Biomechanics and Human Movement Science. Routledge, Abingdon, pp. 197–213.

Durkin, J.L., Dowling, J.J., Andrews, D.M., 2002. The measurement of body segment inertial parameters using dual energy X-ray absorptiometry. J. Biomech. 35, 1575–1580.

Huang, H.K., Suarez, F.R., 1983. Evaluation of cross-sectional geometry and mass density distributions of humans and laboratory animals using computerized tomography. J. Biomech. 16, 821–832.

Lee, M.K., Le, N.S., Fang, A.C., Koh, M.T.H., 2009. Measurement of body segment parameters using dual energy X-ray absorptiometry and three-dimensional geometry: an application in gait analysis. J. Biomech. 42, 217–222.

Martin, P.E., Mungiole, M., Marzke, M.W., Longhill, J.M., 1989. The use of magnetic resonance imaging for measuring segment inertial properties. J. Biomech. 22, 367–376.

McConnell, J., Donnelly, C.J., Hamner, S., Dunne, J., Besier, T., 2011. The effect of shoulder taping on maximum shoulder external and internal rotation in uninjured and previously injured overhead athletes during a seated throw. J. Orthop. Res. 29, 1406–1411.

McConnell, J., Donnelly, C.J., Hamner, S., Dunne, J., Besier, T., 2012. Passive and dynamic shoulder rotation range in uninjured and previously injured overhead athletes and the effect of shoulder taping. PM R 4, 111–116.

McConville, J.T., Churchill, T.D., Kaleps, I., Clauser, C.E., Cuzzi, J., 1980. Anthropometric Relationships of Body and Body Segment Moments of Inertia. AFAMRL-TR-80-119. Aerospace Medical Research Laboratory, Wright-Patterson Air Force Base, Ohio.

Reinbolt, J.A., Seth, A., Delp, S.L., 2011. Simulation of human movement: applications using OpenSim. Procedia IUTAM 2 (0), 186–198.

Rossi, M., Lyttle, A., El-Sallam, A., Benjanuvatra, N., Blanksby, B., 2013. Body segment inertial parameters of elite swimmers using DXA and indirect methods. J. Sport Sci. Med. 12, 761–775.

Wicke, J., Dumas, G.A., 2010. Influence of the volume and density functions within geometric models for estimating trunk inertial parameters. J. Appl. Biomech. 26, 26–31.

Zatsiorsky, V.M., 2002. Kinetics of Human Motion. Human Kinetics, Champaign.